

Mining Maximal Dynamic Spatial Co-Location Patterns

Xin Hu, Guoyin Wang, *Senior Member, IEEE*, and Jiangli Duan

Abstract—A spatial co-location pattern represents a subset of spatial features with instances that are prevalently located together in a geographic space. Although many algorithms for mining spatial co-location patterns have been proposed, the following selected problems remain: 1) these methods miss certain meaningful patterns (e.g., $\{Ganoderma_lucidum_{new}, maple_tree_{dead}\}$ and $\{water_hyacinth_{new}(increase), algae_{dead}(decrease)\}$) and obtain the wrong conclusion if the instances of two or more features increase/decrease (i.e., new/dead) in the same/approximate proportion, which has no effect on the prevalent patterns; 2) because the number of prevalent spatial co-location patterns is quite large, the efficiency of existing methods is low in mining prevalent spatial co-location patterns. Therefore, we first propose the concept of the dynamic spatial co-location pattern that can reflect the dynamic relationships among spatial features. Second, we mine a small number of prevalent maximal dynamic spatial co-location patterns that can derive all prevalent dynamic spatial co-location patterns, which can improve the efficiency of obtaining all prevalent dynamic spatial co-location patterns. Third, we propose an algorithm for mining prevalent maximal dynamic spatial co-location patterns and two pruning strategies. Finally, the effectiveness and efficiency of the proposed method and the pruning strategies are verified by extensive experiments over real/synthetic datasets.

Index Terms—Association rule mining, spatial co-location pattern, dynamic pattern, maximal pattern.

I. INTRODUCTION

SPATIAL co-location pattern mining is an important component of association rule mining [1,2] in machine learning [3,4,5,6]. A spatial co-location pattern represents a subset of spatial features whose instances are prevalently located together in a geographic space. Mining of the spatial co-location pattern is significant. For example, if a city planner cannot find the prevalent pattern $\{school, supermarket, restaurant\}$ near the “school”, this indicates that we need to build a new “supermarket” or “restaurant” around the “school”. Other application domains include public health [7], public transportation [8,9], environmental management [10], social media services [11,12], location services [13,14], and multimedia [15,16,17,18,19], among others.

This work is supported by the Startup Foundation for Introducing Talent of Yangtze Normal University (No. 0107/011160052), the National Key Research and Development Program of China (No. 2016YFB1000901) and the National Natural Science Foundation of China (NSFC, No.61936001, No. 61572091 and No. 61772096). (Corresponding author: Jiangli Duan).

X. Hu is with the College of Big Data and Intelligent Engineering, Yangtze Normal University, Chongqing 408100, China (huxin@yznu.edu.cn).

G. Wang and J. Duan are with the Chongqing Key Laboratory of Computational Intelligence, Chongqing University of Posts and Telecommunications, Chongqing 400065, China (wanggy@cqupt.edu.cn, jl_duan@126.com).

Although many methods for mining spatial co-location patterns exist, they cannot find the dynamic relationships among spatial features. On the one hand, the existing methods miss certain meaningful patterns. Case 1: “*Ganoderma lucidum*” grows on the “*maple tree*”, which was dead. However, existing methods mine patterns from the set of coexisting plants such that the meaningful pattern $\{Ganoderma_lucidum_{new}, maple_tree_{dead}\}$ was missed. Case 2: For mutually inhibitory features such as “*water hyacinth*” and “*algae*”, the instances of “*algae*” decrease with the increase in the instances of “*water hyacinth*” in the same zone. However, because the participation index is always unchanged for existing methods, these methods obtain the prevalent pattern $\{water_hyacinth, algae\}$ regardless of the increase/decrease in instances of “*water hyacinth*”/“*algae*”. On the other hand, existing methods obtain the wrong conclusion that the instances of two or more features increase/decrease (i.e., new/dead) in the same/approximate proportion, which has no effect on prevalent patterns. Case 3: One application of the prevalent spatial co-location pattern judges whether the environment was polluted or not by comparing prevalent patterns at different time points. As shown in Fig. 1, the instances of two features were dead (black shadow) by an equivalent (or approximate) percentage because of environment disruption, but the existing methods determine that the environment has not been polluted because they obtain the same prevalent patterns with the same participation index at two-time points (i.e., t_0 and t_1). In conclusion, finding the dynamic relationships among spatial features (i.e., dynamic spatial co-location patterns) is a promising topic.

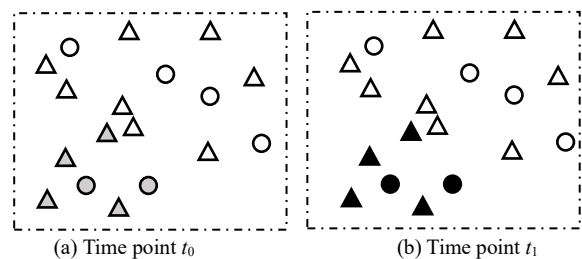


Fig. 1. Sample of case 3

In similar existing methods, the negative/sequential/strong-symbiotic patterns with the above cases appear to be similar, but essential differences exist between them. Both the dynamic pattern and the negative pattern [34,35] can mine mutual exclusion relationship, but the features in the negative pattern cannot coexist. Both the dynamic pattern and the sequential pattern [36,37] are all about time, but the latter is to look for prevalent subsequences from sequential databases. In contrast, the dynamic spatial co-location pattern represents a dynamic relationship between features, which exists in a symbiont circle. The strong-symbiotic pattern [38] belongs to a portion of the dynamic spatial co-location pattern, so it can only mine a portion of the dynamic spatial co-location patterns (i.e., $\{A_{new}, B_{new}\}$) and misses other dynamic spatial co-location patterns (i.e., $\{A_{new}, B_{dead}\}$).

and $\{A_{dead}, B_{dead}\}$).

Moreover, because the amount of spatial data is always quite large, the number of prevalent dynamic spatial co-location pattern is also large, and thus the efficiency of the existing methods is low in mining the prevalent spatial co-location patterns. It is necessary to find certain representative patterns that can derive all prevalent patterns and whose number is small. The prevalent maximal pattern is a compact representation of the prevalent pattern, and the number of prevalent maximal patterns is far less than the number of all prevalent patterns. Therefore, mining the prevalent maximal spatial co-location patterns that can derive all prevalent spatial co-location patterns is more efficient than mining all prevalent spatial co-location patterns using the existing methods. Although selected methods [39,40,41,42,43,44] can mine the prevalent maximal spatial co-location patterns, they still require large numbers of calculations and connections for table instances as well as general methods of mining prevalent spatial co-location patterns.

In summary, the existing methods cannot find the dynamic relationships among spatial features (i.e., dynamic spatial co-location pattern), and the efficiency of mining prevalent dynamic spatial co-location patterns by the existing methods is rather low. Therefore, in this paper, we propose a method for mining the prevalent maximal dynamic spatial co-location pattern and make the following contributions:

1. The existing methods cannot find the dynamic relationships among spatial features, and thus we propose the concept of the dynamic spatial co-location pattern (Dc for short) that can reflect the dynamic relationships among spatial features and can solve the problems in Case 1/Case 2/Case 3.
2. The prevalent maximal patterns can be used to derive all prevalent patterns, and the number of prevalent maximal patterns is far less than the number of all prevalent patterns. Therefore, we mine the prevalent maximal dynamic spatial co-location patterns rather than all prevalent dynamic spatial co-location patterns, which is more efficient than mining all prevalent dynamic spatial co-location patterns using the existing methods.
3. Because a large number of calculations and connections are necessary for table instances in the existing methods for mining maximal patterns, these methods have low efficiency. To improve the efficiency of mining maximal patterns, we propose an algorithm for mining the prevalent maximal dynamic spatial co-location patterns, in which the calculation and connection for table instances are turned into the calculation and connection of dynamic features whose number is far less than that of the instances. Moreover, we propose two pruning strategies to further improve the efficiency.
4. We verified the effectiveness of our algorithm (i.e., we can find the dynamic relationships among spatial features), the representativeness of the prevalent maximal Dc , the efficiency of our algorithm (i.e., comparison with the join-based method), and the efficiency of two pruning strategies over real/synthetic datasets.

II. RELATED WORK

Although many methods for mining spatial co-location pattern have been proposed, no method exists that can mine

the dynamic spatial co-location patterns. S. Shekhar *et al.* [20,21] defined the spatial co-location pattern for the first time and proposed the join-based algorithm. Subsequently, certain methods focused on many other interesting research directions, such as high utility patterns [22,23,24], redundancy reduction [25], improved efficiency [26], causal rules [27], competitive pairs [28], fuzzy objects [29], uncertain data [30,31,32,33], etc. However, the existing methods miss certain meaningful patterns (e.g., $\{Ganoderma_lucidum_{new}, maple_tree_{dead}\}$ and $\{water_hyacinth_{new}(increase), algae_{dead}(decrease)\}$) and obtain the wrong conclusion that the instances of two or more features increase/decrease (i.e., new/dead) in the same/approximate proportion, which has no effect on the prevalent patterns.

The dynamic spatial co-location pattern in this paper might appear to a negative pattern [34,35], sequential pattern [36,37] or strong symbiotic pattern [38], but their essences are different. The features in the negative pattern [34,35] cannot coexist, whereas the features in the dynamic spatial co-location pattern must coexist. Sequential patterns [36,37] represent prevalent repeated paths between items, which exist in the form of a sequence, whereas the dynamic spatial co-location pattern represents a dynamic relationship between features which exist in a symbiont circle. In a strong symbiosis pattern [38], at least one feature benefits from the pattern, so it belongs to a portion of the dynamic spatial co-location pattern, and the method of mining strong symbiosis patterns can only mine a small portion of dynamic spatial co-location patterns (i.e., $\{A_{new}, B_{new}\}$), and other dynamic patterns (i.e., $\{A_{new}, B_{dead}\}$ and $\{A_{dead}, B_{dead}\}$) cannot be mined. In conclusion, the methods for mining a negative pattern, sequential pattern or strong symbiotic pattern cannot mine the dynamic spatial co-location pattern in this paper.

TABLE I
CATEGORY OF METHODS

Categories	Innovations	Literatures
Traditional co-location pattern	Origin	[20,21]
	high utility patterns	[22,23,24]
	redundancy reduction	[25]
	improved efficiency	[26]
	causal rules	[27]
	competitive pairs	[28]
	fuzzy objects	[29]
Similar methods	uncertain data	[30,31,32,33]
	Negative pattern	[34,35]
	Sequential pattern	[36,37]
Related methods	Strong-symbiotic	[38]
	maximal pattern	[39,40,41,42,43,44]

Although certain methods can mine the prevalent maximal spatial co-location pattern, they still require a large number of calculations and connections for table instances as well as general methods of mining prevalent spatial co-location patterns. Wang *et al.* [39] proposed an order-clique-based approach for mining maximal co-location pattern, and based on this approach, Yao *et al.* [40,41] proposed an ordered-instance-clique approach. Dai *et al.* [42] used an index structure similar to four binary trees to mine the maximal spatial co-location patterns. Bao *et al.* [43] mined the top- k longer size maximal co-location patterns. Wang *et al.* [44] mined the maximal sub-prevalent co-location patterns, which introduced star participation instances to measure the prevalence of co-location patterns, i.e., spatially correlated

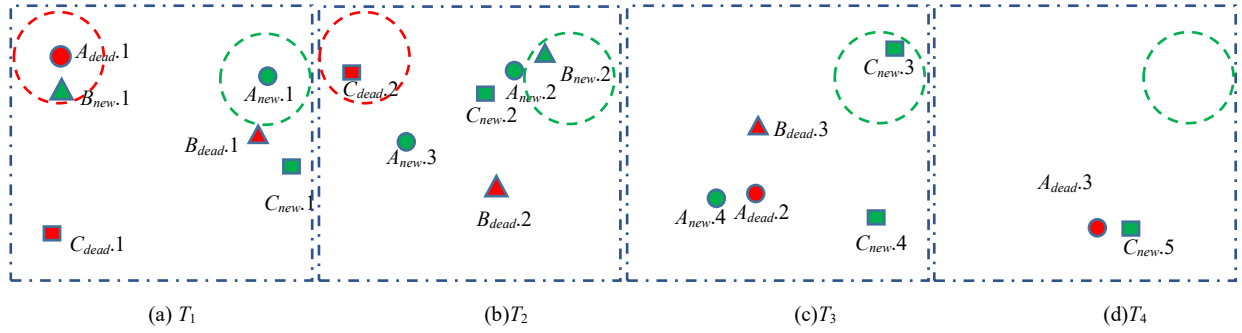


Fig. 2. Sample distribution datasets of new/dead instance

instances that cannot form cliques were also properly considered. However, the above methods still require a large number of calculations and connections for table instances. In contrast, we propose an algorithm for mining prevalent maximal dynamic spatial co-location patterns, which is based on a degree-based approach for the maximum clique/maximal co-location patterns [45,46] and turns the calculation and connection for table instances into calculation and connection of dynamic features, the number of which is far less than that of instances.

III. BASIC DEFINITIONS

Definition 1. (Dynamic Feature/Instance) A dynamic feature represents the new/dead object in a certain area, denoted as $Df_{[i]}$, which is a new or dead object (e.g., A_{new} , A_{dead} are two dynamic features in Fig. 2). A dynamic instance is an instance of a dynamic feature at a specific location, denoted as $Df_{[i].j}$ (e.g., $A_{new.1}$ and $A_{new.2}$ are two instances of the dynamic feature A_{new} in Fig. 2).

Definition 2. (Dynamic Distance Threshold, D_d) If the distance between two dynamic instances is less than D_d as designated by experts, it is considered that the two dynamic instances have a relationship, and otherwise, they have no relationship.

Definition 3. (Time Span and Time Span Constraint) *Time span* is the time difference between two adjacent dynamic datasets and represents the time interval in which certain instances have changed, which is designated by experts. The *time span constraint* of a dynamic feature is the length of time in which the feature influences the surrounding dynamic features, denoted as $span(Df_{[i]})$. Furthermore, if the *time span constraint* of $Df_{[i]}$ is equal to k time spans, it can be represented as $span(Df_{[i]}) = k$ (*time spans*).

The effect of a new object $Df_{[i]}$ on the surrounding dynamic features is the life cycle of $Df_{[i]}$. For example, we assume that the *time span* is 3 years and that the life cycle of A_{new} is 75 years, and thus $span(A_{new}) = 25(\text{time spans})$.

The effect of a dead object $Df_{[i]}$ on the surrounding dynamic features is a *one-time span* because the dead object has little effect on the surrounding dynamic features, and the *one-time span* can sufficiently cover the time interval in which a dead object influences the surrounding instances. Thus $span(A_{dead}) = 1(\text{time span})$.

Definition 4. (Dynamic Spatial Neighborhood Relationship, D_R) For two dynamic instances, if the distance between them is less than D_d , which is designated by experts, and the time difference between them is less than the maximum of the *time span constraints* of all dynamic features, it is considered that the two dynamic instances satisfy the dynamic spatial neighborhood relationship D_R .

$$D_R(A_{new.1}, B_{dead.2}) \Leftrightarrow \text{distance}(A_{new.1}, B_{dead.2}) \leq D_d$$

and

$$\Delta T(A_{new.1}, B_{dead.2}) < \max(\text{span}(A_{new}), \text{span}(B_{dead}))$$

Definition 5. (Dynamic Spatial Co-Location Pattern, D_c) A dynamic spatial co-location pattern contains multiple new/dead features and can reflect the dynamic relationships among dynamic features, denoted as D_c . For example, $Dc_{[i]} = \{A_{new}, B_{dead}\}$ is a size-2 dynamic spatial co-location pattern.

Definition 6. (Dynamic Row Instance and Dynamic Table Instance) For a dynamic spatial co-location pattern D_c and a set of dynamic instances DI , if a one-to-one match exists between each dynamic instance in DI and each dynamic feature in D_c and any two dynamic instances in DI satisfy the dynamic spatial neighborhood relationship, we say that DI is a dynamic row-instance of D_c , denoted as dynamic row-instance (Dc). The dynamic table-instance of D_c consists of all distinct dynamic row-instances of D_c , denoted as dynamic table-instance (Dc).

Example 1. For $Dc_{[i]} = \{A_{new}, B_{new}\}$, if both $(A_{new.1}, B_{new.2})$ and $(A_{new.2}, B_{new.2})$ satisfy the dynamic spatial neighborhood relationship, they are the dynamic row-instance of $Dc_{[i]}$, and $\{\{A_{new.1}, B_{new.2}\}, \{A_{new.2}, B_{new.2}\}\}$ is the dynamic table-instance of $Dc_{[i]}$, denoted as dynamic table-instance($Dc_{[i]}$) = $\{\{A_{new.1}, B_{new.2}\}, \{A_{new.2}, B_{new.2}\}\}$.

Definition 7. (Dynamic Participation Ratio (DPR)/ Index (DPI)) The dynamic participation ratio $DPR(Dc, Df_{[i]})$ of dynamic feature $Df_{[i]}$ in a size- k dynamic spatial co-location pattern $Dc = \{Df_{[1]}, Df_{[2]} \dots Df_{[k]}\}$ is defined as follows:

$$DPR(Dc, Df_{[i]}) = \frac{\pi_{Df_{[i]}}(\text{dynamic_table_instance}(Dc))}{\text{dynamic_table_instance}(\{Df_{[i]}\})}$$

where π is the relational projection operation with a duplication elimination. $DPI(Dc)$ of Dc is defined as shown:

$$DPI(Dc) = \min_{i=1}^k \{DPR(Dc, Df_{[i]})\}$$

If $DPI(Dc)$ is greater than a given minimum prevalence threshold min_prev that is designated by experts and is used to judge whether the pattern occurs prevalently or not, we say that Dc is a prevalent dynamic spatial co-location pattern.

Example 2. For $Dc_{[i]} = \{A_{new}, B_{new}\}$, dynamic table-instance($Dc_{[i]}$) = $\{\{A_{new.1}, B_{new.2}\}, \{A_{new.2}, B_{new.2}\}\}$. In $Dc_{[i]}$, the number of dynamic instances of A_{new} and B_{new} are 2 and 1, respectively. In contrast, from Fig. 2, the total number of dynamic instances of A_{new} and B_{new} are 4 and 2, respectively. Therefore, $DPR(Dc_{[i]}, A_{new}) = 2/4 = 0.5$, $DPR(Dc_{[i]}, B_{new}) = 1/2 = 0.5$ and thus $DPI(Dc_{[i]}) = \min\{DPR(Dc_{[i]}, A_{new}), DPR(Dc_{[i]}, B_{new})\} = 0.5$. If $min_prev = 0.3$, $Dc_{[i]} = \{A_{new}, B_{new}\}$ is a size-2 prevalent dynamic spatial co-location pattern.

Definition 8. (Prevalent Maximal Dynamic Spatial Co-Location Pattern) Given a prevalent dynamic spatial co-location pattern $Dc = \{Df_{[1]}, \dots, Df_{[v]}\}$, for any $Df_{[i]} \in Df$ and

$Df_{[i]} \notin Dc$, if any $Dc \cup Df_{[i]}$ is not a prevalent dynamic spatial co-location pattern, then Dc is a prevalent maximal dynamic spatial co-location pattern.

Definition 9. (Dynamic Spatial Feature Clique, Dfc) Given a dynamic spatial feature set $Dfc = \{Df_{[1]}, \dots, Df_{[n]}\}$, if any size-2 pattern $Dc_{[i]} = \{Df_{[j]}, Df_{[k]}\}$ ($Df_{[j]}, Df_{[k]} \in Dfc$ and $j \neq k$) is prevalent, then Dfc is a dynamic spatial feature clique.

Definition 10. (Maximal Dynamic Spatial Feature Clique) Given a dynamic spatial feature set $Dfc = \{Df_{[1]}, \dots, Df_{[n]}\}$, for any $Df_{[i]} \in Df$ and $Df_{[i]} \notin Dfc$, if $Dfc \cup Df_{[i]}$ is not a dynamic spatial feature clique, then Dfc is a maximal dynamic spatial feature clique.

IV. MINING PREVALENT MAXIMAL Dc (ALGORITHM MDC)

We propose an algorithm for mining the prevalent maximal dynamic spatial co-location pattern (i.e., Algorithm MDC), which is divided into three sub algorithms (i.e., *Algorithm 1*, *Algorithm 2*, *Algorithm 3*). For convenience of description, the dynamic spatial co-location pattern is abbreviated as Dc in this paper.

Because a large number of calculations and connections exist for table instances in the existing methods, these methods have low efficiency. To improve the efficiency of mining patterns, after obtaining the size-2 prevalent dynamic spatial co-location patterns, we convert them to a dynamic feature graph DG by *Algorithm 1* such that the calculation and connection for the table instances are turned into the calculation and connection of the dynamic features. Subsequently, we obtain the set of maximal dynamic feature clique Dfc from the dynamic feature graph DG by *Algorithm 2*. Finally, each maximal dynamic feature clique Dfc as a candidate maximal Dc is verified by *Algorithm 3*, and thus we can obtain prevalent maximal Dc .

A. First Sub-Algorithm

First, we generate the distribution dataset of dynamic instances (i.e., new/dead instances) from the distribution dataset of spatial instances at different time points (*step 1* and *Example 3*). Second, with D_d , *time span* and *time span constraint* (i.e., life cycle) of each dynamic feature, we can confirm whether any two dynamic instances have a dynamic spatial neighborhood relationship or not and obtain a set of all dynamic neighborhood relationships (*step 2* and *Example 4*). Second, we obtain the dynamic table-instance of all size-2 Dc by arranging all dynamic neighborhood relationships, and thus we obtain the size-2 prevalent Dc by definition 8 and *min_prev* (*step 3/step 4* and *Example 5*). Finally, we transform all size-2 prevalent Dc to dynamic feature graph DG (*step 5* and *Example 6*).

Algorithm 1: Generating Dynamic Feature Graph DG

Input: (1) $Df = \{Df_{[1]}, Df_{[2]}, \dots, Df_{[n]}\}$: a set of dynamic spatial features; (2) $St = \{St_{[1]}, St_{[2]}, \dots, St_{[n]}\}$: the distribution dataset of spatial instances at different time points; (3) $Lc = \{Lc_{[1]}, Lc_{[2]}, \dots, Lc_{[n]}\}$: a set of life cycle of all dynamic features; (4) D_d : a dynamic distance threshold; (5) min_prev : a minimum DPI threshold.

Output: DG : dynamic feature graph.

Variables: S_T : the distribution dataset of dynamic instances at different time points.

- 1: $S_T = \text{Gen_dynamic_instance_distribution}(St)$
 - 2: $\delta_{DR} = \text{Gen_dynamic_neighborhood}(Df, S_T, D_d, Lc, \text{time_span})$
 - 3: $\delta_{dynamic_table_instance} = \text{Gen_dynamic_table_instance}(Df, \delta_{DR})$
 - 4: $\delta_{dynamic_size2_prevalent_Dc}(Df, \delta_{dynamic_table_instance}, min_prev)$
 - 5: $DG = \text{Gen_dynamic_feature_graph}(\delta_{dynamic_size2})$
-

Example 3. Given the distribution dataset of spatial instances at different time points (i.e., t_1, t_2, \dots, t_n), because this paper studies the dynamic relationship among features, we obtain $n-1$ dynamic datasets that contain only new/dead instances by comparing two datasets at t_i and t_{i+1} . For instance, we can obtain a dynamic dataset in Fig. 2(a) by comparing the two datasets at t_1 and t_2 . The new/dead (green/red in Fig. 2) categorizations of the same object are denoted by two dynamic features (i.e., A_{new}/A_{dead}), respectively. One instance of feature A exists in t_1 and disappears at t_2 , and it is used as a dead instance in T_1 , denoted by $A_{dead.1}$. Similarly, if one instance of feature A appears at t_2 for the first time, it is used as a new instance in T_1 , denoted by $A_{new.1}$. As shown in Fig. 2, the distribution datasets of new/dead instances are obtained by comparing the datasets at 5 time points.

Example 4. Suppose $D_d = k$ and $span(A_{new}) = 3(\text{time spans})$ (the time difference between T_1 and T_2 is one *time span*). To obtain the neighborhood instances of $A_{new.1}$ in Fig. 2(a), we should confirm whether $A_{new.1}$ and all other dynamic instances in Fig. 2(a)(b)(c)(d) (according to definition 3 and $span(A_{new}) = 3(\text{time spans})$) satisfy the dynamic spatial neighborhood relationship or not by definition 4. Subsequently, we determine that $B_{new.2}$ and $C_{new.3}$ are the neighborhood instances of $A_{new.1}$. Similarly, to obtain the neighborhood instances of $A_{dead.1}$ in Fig. 2(a), we should confirm whether $A_{dead.1}$ and all other dynamic instances in Fig. 2(a)(b) (according to definition 3, and thus $span(A_{dead}) = 1(\text{time span})$) satisfy the dynamic spatial neighborhood relationship or not by definition 4. Finally, we find that $B_{new.1}$ and $C_{dead.2}$ are the neighborhood instances of $A_{dead.1}$.

Example 5. By arranging all neighborhood dynamic instance pairs of A_{new} and B_{new} (i.e., $A_{new.1}$ and $A_{new.2}$ are the neighborhood dynamic instances of $B_{new.2}$), we obtain the dynamic table-instances $\{\{A_{new.1}, B_{new.2}\}, \{A_{new.2}, B_{new.2}\}\}$ of $Dc_{[i]} = \{A_{new}, B_{new}\}$. Suppose $min_prev = 0.3$ according to definition 7, because $DPI(Dc_{[i]}) = 0.5 > 0.3$, and thus $Dc_{[i]} = \{A_{new}, B_{new}\}$ is a size-2 prevalent Dc .

Example 6. Suppose certain size-2 prevalent dynamic spatial co-location patterns exist such as $\{A_{new}, B_{new}\}$, $\{A_{new}, C_{new}\}$, $\{A_{dead}, B_{new}\}$, $\{A_{dead}, B_{dead}\}$, $\{A_{dead}, C_{dead}\}$ and $\{B_{new}, C_{dead}\}$. In Fig. 3, each dynamic feature in all size-2 prevalent Dc and each size-2 prevalent Dc are treated as a vertex and an edge, respectively. For instance, because $\{A_{new}, B_{new}\}$ is a size-2 prevalent Dc , we should connect A_{new} and B_{new} . In contrast, A_{new} does not connect to C_{dead} because $\{A_{new}, C_{dead}\}$ is not a prevalent Dc . Finally, we obtain a dynamic feature graph DG , as shown in Fig. 3.

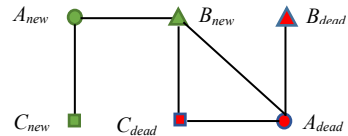


Fig. 3. Sample dynamic feature graph

B. Second Sub-Algorithm

The maximal Dfc (dynamic feature clique) is treated as the candidate prevalent maximal Dc and can be obtained from DG by *Algorithm 2*, which is proposed based on the degree-based approach for the maximum clique/maximal co-location patterns [45,46].

The core idea of *Algorithm2* is described as follows. First, the vertex with maximum degree in DG is selected as V_{max} , and other vertices are divided into two categories (adjacent and non-adjacent vertices). Second, V_{max} is treated as a node in one candidate Dfc , and all of the adjacent vertices of V_{max} form a subgraph (i.e., $sub_DG_{[1]}$). This process is applied recursively for $sub_DG_{[1]}$. Third, the non-adjacent vertices of V_{max} are treated successively as V_{max}' , which is the same as V_{max} . For i -th V_{max}' , the adjacent vertices of V_{max}' form a subgraph (i.e., $sub_DG_{[2i]}$), and $sub_DG_{[2i]}$ is subjected to a recursive process similar to that of $sub_DG_{[1]}$.

In the recursive process, starting from the vertex with maximum degree (V_{max}) can accelerate the speed of finding all maximal Dfc . Because each vertex in the maximal Dfc must connect to all other vertices in the maximal Dfc , V_{max} is always located in a maximal Dfc that contains many vertices. On the one hand, starting from V_{max} can quickly reduce the edges in $sub_DG_{[1]}$, and thus it accelerates the process of finding the maximal Dfc in $sub_DG_{[1]}$. On the other hand, starting from V_{max} always first finds the maximal Dfc that contains many vertices such that $sub_DG_{[2]}$ is far less than original DG , and therefore, it can accelerate the process of finding the maximal Dfc in $sub_DG_{[2]}$.

Algorithm 2: Generating Maximal Dynamic Feature Clique

Input: DG : dynamic feature graph.
Output: $\delta_{maximal_dynamic_clique}$: the set of maximal Dfc .
Variables: (1) Df : a set of dynamic spatial features; (2) can_Dfc : a set of candidate vertices in dynamic feature cliques; (3) V_{max} : a vertex with max degree; (4) $link_Df$: a set of adjacent vertices of V_{max} ; (5) not_link_Df : a set of non-adjacent vertices of V_{max} ; (6) V_{max}' : vertex in not_link_Df is regarded as V_{max}' successively, which is the same as V_{max} ; (7) $second_Df$: a set of adjacent vertices of V_{max}' .
 Clique (Df, can_Dfc, DG)
 1: $V_{max} = \text{Get_maxdegree_Df}(Df, DG)$
 2: $link_Df, not_link_Df = \text{Get_link_or_unlink_Vmax}(Df, DG)$
 3: If (Exist_side ($link_Df$))
 Clique ($link_Df, can_Dfc + V_{max}, DG$)
 Else
 $\delta_{maximal_dynamic_clique} + (can_Dfc + V_{max} + link_Df)$
 4: While (Exist_dynamic_feature (not_link_Df, DG))
 $V_{max}' = \text{Get_and_delete_first_Df}(not_link_Df, DG)$
 $second_Df = \text{Get_link_Vmax}'(not_link_Df, link_Df, DG)$
 If (Exist_side ($second_Df, DG$))
 Clique ($second_Df, can_Dfc + V_{max}', DG$)
 Else
 $\delta_{maximal_dynamic_clique} + (can_Dfc + V_{max}' + second_Df)$

Example 7. For DG in Fig. 3, $V_{max[1]} = B_{new}$, and other vertices can be divided into adjacent/non-adjacent vertices. For the adjacent portion of B_{new} , B_{new} is treated as one node in the candidate maximal Dfc (i.e., $can_Dfc = \{B_{new}\}$), and the adjacent vertices form a subgraph (i.e., $sub_DG_{[1]} = \{A_{new}, A_{dead}, C_{dead}\}$). *Algorithm2* executes a recursion process for $sub_DG_{[1]}$, $V_{max[11]} = A_{dead}$, and for the adjacent portion of A_{dead} , A_{dead} is treated as one node in candidate maximal Dfc (i.e., $can_Dfc = \{B_{new}, A_{dead}\}$), and the adjacent vertices form a subgraph (i.e., $sub_DG_{[11]} = \{C_{dead}\}$). Because no edge exists in $sub_DG_{[11]}$, *Algorithm2* adds the remaining nodes to the candidate maximal Dfc and obtains the first maximal Dfc (i.e., $Dfc_{[1]} = \{B_{new}, A_{dead}, C_{dead}\}$). For the non-adjacent portion of A_{dead} , the candidate maximal Dfc is $\{B_{new}\}$, and no edge exists in $sub_DG_{[12]} = \{A_{new}\}$. Similarly, we obtain the second maximal Dfc (i.e., $Dfc_{[2]} = \{B_{new}, A_{new}\}$). For the non-adjacent vertices (i.e., C_{new} and B_{dead}) of B_{new} , the candidate maximal Dfc is $\{C_{new}\}$, C_{new} and B_{dead} are successively treated as V_{max}' , and their adjacent vertices form subgraphs $sub_DG_{[21]} = \{A_{new}\}$ and $sub_DG_{[22]} = \{A_{dead}\}$, respectively. Thus, we can obtain

$Dfc_{[3]} = \{C_{new}, A_{new}\}$ and $Dfc_{[4]} = \{B_{dead}, A_{dead}\}$. Finally, we can obtain all maximal Dfc (i.e., $\{B_{new}, A_{dead}, C_{dead}\}$, $\{B_{new}, A_{new}\}$, $\{C_{new}, A_{new}\}$ and $\{B_{dead}, A_{dead}\}$).

C. Third Sub-Algorithm

Each maximal Dfc is treated as a candidate maximal Dc (i.e., $Dc_{[i]}$); therefore, we need to verify whether it is prevalent or not. First, we obtain the dynamic table instance of the candidate maximal $Dc_{[i]}$, which can be obtained by the dynamic table-instance of the size-2 prevalent Dc (*Example 8*). Second, we calculate the DPI of the candidate maximal $Dc_{[i]}$ and compare it with min_prev . Third, if the $Dc_{[i]}$ is prevalent, we add it to the set of prevalent maximal Dc ; otherwise, it is decomposed into a size- k -1 pattern ($Dc_{[i]}$ is a size- k pattern) (*Example 9*), and each size- k -1 pattern is treated as a candidate maximal Dc and passes through a verification process (except the one that already exists in the set of prevalent maximal Dc).

Algorithm 3: Verifying Prevalent Maximal Spatial Co-Location Pattern

Input: (1) $\delta_{maximal_Dfc}$: the set of maximal Dfc which is regarded as candidate prevalent maximal Dc ; (2) min_prev : minimum prevalent threshold; (3) $\delta_{size2_prevalent}$: size-2 prevalent Dc .
Output: $\delta_{prevalent_dynamic_maximal_Dc}$: the set of prevalent Dc .
Variables: (1) $clique$: one maximal Dfc ; (2) $Df_{[n]}$: a set of dynamic features in clique; (3) $\delta_{clique_size2_prevalent}$: a set of dynamic table instances of size-2 prevalent Dc which contains $Df_{[0]}$; (4) $common_instance$: common instances of $Df_{[0]}$ in size-2 prevalent Dc which contains $Df_{[0]}$; (5) δ_{cci} : validated dynamic table instance of Dfc ; (6) δ_{size_k-1} : a set of size- k -1 subpatterns of Dfc .
 While (not_empty($\delta_{maximal_Dfc}$))
 1: $clique = \text{Get_one_clique}(\delta_{maximal_Dfc})$
 2: $Df_{[n]} = \text{Get_dynamic_feature}(clique)$
 3: for ($i = 1; i < n; i++$)
 $\delta_{clique_size2_prevalent} = \text{Get_dynamic_table_instance}(Df_{[0]}, Df_{[i]}, \delta_{size2_prevalent})$
 4: $common_instance = \text{Get_common_instance_Df}_{[0]}(\delta_{clique_size2_prevalent})$
 5: $\delta_{cci} = \text{Get_clique_dynamic_instance}(common_instance, \delta_{clique_size2_prevalent})$
 6: for ($i = 1; i < n - 1; i++$)
 for ($j = i + 1; j < n; j++$)
 $\delta_{cci} = \text{Verifying}(\delta_{cci}, \delta_{clique_dynamic_size2}, Df_{[i]}, Df_{[j]})$
 7: If (prevalently(δ_{cci}))
 $\delta_{prevalent_dynamic_maximal_Dc} = \delta_{prevalent_dynamic_maximal_Dc} + clique$
 8: Else if (size ($clique$) > 3)
 $\delta_{size_k-1} = \text{Split}(clique)$
 $\delta_{size_k-1} = \text{Non_prevalent}(\delta_{size_k-1}, \delta_{prevalent_dynamic_maximal_Dc}, \delta_{maximal_Dfc})$
 $\delta_{maximal_Dfc} = \delta_{maximal_Dfc} + \delta_{size_k-1}$

Example 8. Given the maximal Dfc , which is also a candidate maximal Dc (i.e., $Dc_{[i]} = \{A_{dead}, B_{new}, C_{dead}\}$), we first obtain the common instances from the dynamic table instances of selected size-2 prevalent subpatterns (i.e., $Dc_{[i1]} = \{A_{dead}, B_{new}\}$ and $Dc_{[i2]} = \{A_{dead}, C_{dead}\}$). For example, from the dynamic table-instance ($Dc_{[i1]} = \{\{A_{dead}.1, B_{new}.1\}, \{A_{dead}.1, B_{new}.2\}, \{A_{dead}.2, B_{new}.1\}\}$) and the dynamic table-instance ($Dc_{[i2]} = \{\{A_{dead}.1, C_{dead}.2\}\}$), we can obtain the common instances (i.e., $A_{dead}.1$) of $Dc_{[i1]}$ and $Dc_{[i2]}$. Second, with the common dynamic instances, we select the dynamic row-instances of the size-2 prevalent subpatterns to construct the candidate dynamic row-instances of $Dc_{[i]}$. For example, with $A_{dead}.1$, we select the dynamic row-instances set $\{\{A_{dead}.1, B_{new}.1\}, \{A_{dead}.1, B_{new}.2\}\}$ and $\{\{A_{dead}.1, C_{dead}.2\}\}$ and subsequently construct the dynamic row-instances of $Dc_{[i]}$ (i.e., $\{A_{dead}.1, B_{new}.1, C_{dead}.2\}$ and $\{A_{dead}.1, B_{new}.2, C_{dead}.2\}$). Third, we verify the dynamic row-instances by the other size-2 prevalent subpattern (i.e., $Dc_{[i3]} = \{B_{new}, C_{dead}\}$). For example, because only the dynamic row-instance $\{B_{new}.1, C_{dead}.2\}$ exists in the dynamic table-instance of $Dc_{[i3]}$ while another dynamic row-instance $\{B_{new}.2, C_{dead}.2\}$ does not exist, only $\{A_{dead}.1, B_{new}.1, C_{dead}.2\}$ is a real dynamic

row-instance of $Dc_{[i]}$, and thus we obtain the dynamic table-instance $(Dc_{[i]} = \{A_{dead.1}, B_{new.1}, C_{dead.2}\})$.

Example 9. Supposing that a size-4 candidate Dc (i.e., $Dc_{[i]} = \{A_{dead}, B_{new}, C_{dead}, D_{new}\}$) is not prevalent, we divide the Dc into size-3 candidate Dc (i.e., $\{A_{dead}, B_{new}, C_{dead}\}$, $\{A_{dead}, B_{new}, D_{new}\}$, $\{A_{dead}, C_{dead}, D_{new}\}$ and $\{B_{new}, C_{dead}, D_{new}\}$). If candidate pattern $\{A_{dead}, B_{new}, C_{dead}\}$ already exists in the set of prevalent maximal Dc , then it is deleted from the set of subpatterns. We add the size-3 candidate patterns $\{A_{dead}, B_{new}, D_{new}\}$, $\{A_{dead}, C_{dead}, D_{new}\}$ and $\{B_{new}, C_{dead}, D_{new}\}$ to the set of candidate Dc .

V. PRUNING STRATEGIES

Theorem 1. For a dynamic feature $Df_{[j]}$ in the candidate prevalent maximal $Dc_{[i]}$, if $DPR(Dc_{[i]}, Df_{[j]}) < \min_prev$, then $Dc_{[i]}$ is non-prevalent.

Proof. From definition 7, $DPI(Dc_{[i]})$ is the minimum value among dynamic participation ratios of all dynamic features in $Dc_{[i]}$. Therefore, if $DPR(Dc_{[i]}, Df_{[j]}) < \min_prev$, then $DPI(Dc_{[i]}) \leq DPR(Dc_{[i]}, Df_{[j]}) < \min_prev$, namely, $Dc_{[i]}$ is non-prevalent.

Pruning Strategy 1. During verification of a candidate prevalent maximal Dc , if the dynamic participation ratio of any dynamic feature is smaller than \min_prev , then we can stop verification and confirm that the candidate maximal Dc is nonprevalent.

Example 10. During verification of the size-4 candidate prevalent maximal Dc (i.e., $Dc_{[i]} = \{A_{dead}, B_{new}, C_{dead}, D_{new}\}$), we can calculate the dynamic participation ratio of any dynamic feature in the process of obtaining the common instances of A_{dead} and verifying the dynamic row-instance of $Dc_{[i]}$. If $DPR(Dc_{[i]}, A_{dead}) < \min_prev$, then we can stop verification and confirm that $Dc_{[i]}$ is non-prevalent.

Theorem 2. Given a candidate prevalent maximal $Dc_{[i]}$ and its superpattern $Dc_{[i]'}$ (i.e., $Dc_{[i]} \subseteq Dc_{[i]'}$ and $Dc_{[i]} \neq Dc_{[i]'}$), if $Dc_{[i]}$ is non-prevalent, then $Dc_{[i]'}$ is also non-prevalent.

Proof. Pattern $Dc_{[i]}$ is non-prevalent, and we know that a dynamic feature $Df_{[j]} \in Dc_{[i]}$ exists and $DPR(Dc_{[i]}, Df_{[j]}) < \min_prev$. Therefore, for its superpattern $Dc_{[i]'}$ (i.e., $Dc_{[i]} \subseteq Dc_{[i]'}$ and $Dc_{[i]} \neq Dc_{[i]'}$), the existence of inheritance leads to $DPR(Dc_{[i]'}, Df_{[j]}) \leq DPR(Dc_{[i]}, Df_{[j]}) < \min_prev$, and thus $Dc_{[i]'}$ is non-prevalent.

Pruning Strategy 2. If multiple candidate prevalent maximal dynamic spatial co-location patterns have a common subpattern, we can first verify their common subpattern, and if the common subpattern is non-prevalent, all candidate prevalent maximal spatial co-location patterns are non-prevalent.

Example 11. Given a candidate prevalent maximal dynamic spatial co-location patterns $Dc_{[i]} = \{A_{dead}, B_{new}, C_{dead}, D_{new}\}$ and $Dc_{[j]} = \{A_{dead}, B_{new}, C_{dead}, E_{dead}\}$, we can first verify the common subpattern $Dc_{[i][j]} = \{A_{dead}, B_{new}, C_{dead}\}$, and if $Dc_{[i][j]}$ is non-prevalent, then both $Dc_{[i]}$ and $Dc_{[j]}$ are non-prevalent. If $Dc_{[i][j]}$ is prevalent, then we verify the other portions of $Dc_{[i]}$ and $Dc_{[j]}$.

VI. COMPLEXITY ANALYSIS

To analyze the complexity, the upper limits of certain parameters will need to be determined. For the original datasets (i.e., n time points), the number of instances at each time point is no more than I . For the dynamic datasets (i.e., $n-1$ time points), the number of dynamic instances in each dynamic dataset is I' , and there are $2 * F$ dynamic features

(new/dead). For any dynamic feature, its dynamic instances and *time span constraint* are no more than i and n , respectively.

A. Time Complexity

In *Algorithm1*, from step 1 to step 5, the corresponding complexities are $O(I * I * (n-1))$, $O(I^2 * (n-1)^2)$, $O(I^2 * (n-1)^2 / 2)$, $O(F * F)$ and $O(F * F)$, and thus the time complexity of *Algorithm1* is $O(I^2 * n) + O(I^2 * n^2)$, where F is much less than I , so selected portions have been omitted. In *Algorithm2*, for any dynamic feature $Df_{[j]}$, the number of dynamic feature cliques that are related to $Df_{[j]}$ is no more than F , and there are $2 * F$ dynamic features. Therefore, the number of dynamic feature cliques is no more than $F * 2 * F$. Moreover, from the literature [45], the time complexity of obtaining a maximum clique is $O(1.442^F)$, and thus the time complexity of *Algorithm2* is $O(1.442^{F * F})$. In *Algorithm3*, the number of dynamic feature cliques is $F * 2 * F$ (from *Algorithm2*), any dynamic feature clique is decomposed once (on average), and therefore, its number is no more than $F * 2 * F * F$ after decomposition. Moreover, for one dynamic feature clique, the time complexity of verification is $O(F^2)$, so the time complexity of *Algorithm3* is $O(F^5)$. Therefore, the time complexity of Algorithm MDC is $O(I^2 * n) + O(I^2 * n^2) + O(1.442^{F * F}) + O(F^5)$.

B. Space Complexity

The space complexity values of the storing instances, dynamic features, dynamic instances, adjacent instance set, dynamic table-instances, dynamic feature graph, dynamic feature cliques, common code and decomposed maximal cliques are $O(I * n)$, $O(2 * F)$, $O(I * (n-1))$, $O(I^2 * (n-1)^2 / 2)$, $O(I^2 * (n-1)^2 / 2)$, $O(F * F)$, $O(F * 2 * F)$, $O(i)$ and $O(F)$, respectively. Moreover, during searching of the dynamic feature clique, the space complexity is $O(F^2)$. Therefore, the space complexity of Algorithm MDC is $O(I * n) + O(I^2 * n^2) + O(F * 2 * F)$, where I' , I and F are much less than I , $I' * n$ and I , respectively, and thus certain portions have been omitted.

VII. EXPERIMENTAL EVALUATION

Various experiments over both real and synthetic datasets were conducted to verify the effectiveness of Algorithm MDC (i.e., we can find the dynamic relationships among spatial features), the representativeness of the prevalent maximal Dc , the efficiency of Algorithm MDC (i.e., comparison with the join-based algorithm), and the efficiency of the two pruning strategies.

A. Experiments on Real Dataset

In this section, we verify the effectiveness of the Algorithm MDC, namely, whether the Algorithm MDC can mine the dynamic relationships among spatial features (i.e., Dc) from the real datasets.

The real dataset is sourced from the Wuhua district of Kunming, Yunnan province, China, in the most recent 30 years. Specifically, $Df = \{\text{"School"}, \text{"Park"}, \text{"Hospital"}, \text{"Hotel"}, \text{"Supermarket"}, \text{"KTV"}, \text{"Bank"}\}$, where "Bank" includes bank business halls and ATMs, and "Hospital" includes clinics, pharmacies, etc. The *life cycle* of all dynamic feature is $\{30, 30, 15, 9, 6, 6, 6\}$, the number of new/dead instances is approximately 1500, and the *time span* is 3 years. If D_d is 1 km and \min_prev is 0.4, we can obtain all prevalent Dc as shown in Table II, which can be derived from the prevalent maximal Dc .

TABLE II
PREVALENT DYNAMIC SPATIAL CO-LOCATION PATTERNS

	A_{new}, B_{new}	A_{dead}, B_{dead}	A_{new}, B_{dead}
size-2	$\{school_{new}, supermarket_{new}\}$ $\{school_{new}, bank_{new}\}$ $\{school_{new}, KTV_{new}\}$ $\{KTV_{new}, bank_{new}\}$ $\{hospital_{new}, bank_{new}\}$ $\{hospital_{new}, supermarket_{new}\}$ $\{hotel_{new}, bank_{new}\}$ $\{hotel_{new}, KTV_{new}\}$ $\{part_{new}, hotel_{new}\}$	$\{school_{dead}, bank_{dead}\}$ $\{hospital_{dead}, supermarket_{dead}\}$ $\{hotel_{dead}, bank_{dead}\}$ $\{hotel_{dead}, KTV_{dead}\}$ $\{KTV_{dead}, bank_{dead}\}$	$\{hotel_{dead}, supermarket_{new}\}$ $\{supermarket_{new}, KTV_{dead}\}$ $\{hospital_{new}, KTV_{dead}\}$ $\{school_{new}, KTV_{dead}\}$
size-3	$\{hotel_{new}, KTV_{new}, bank_{new}\}$	$\{hotel_{dead}, KTV_{dead}, bank_{dead}\}$	$\{hotel_{dead}, supermarket_{new}, KTV_{dead}\}$

Traditional methods can obtain the prevalent pattern {"School", "Park", "Hospital", "Hotel", "Supermarket", "KTV", "Bank"} at each time point (i.e., $t_0, t_1, t_2, \dots, t_n$) when $D_d=1$ km and $min_prev=0.4$, namely, all features are always coexistent at each time point, and the result is not meaningful. In contrast, from the experimental results of Algorithm MDC in Table II, we can obtain the following meaningful information:

- 1) The instances of "Bank" increase (or decrease) with the increase (or decrease) of the instances of "School", "Hotel", "Hospital" and "KTV", which means that Algorithm MDC can find the dynamic relationships among spatial features such as $\{water_hyacinth_{new}(\text{increase}), algae_{dead}(\text{decrease})\}$.
- 2) Life service (e.g., "Hospital" and "Supermarket") has a mutual exclusion relationship with entertainment (e.g., "KTV"), namely, the instances of "Hospital" and "Supermarket" increase (or decrease) with the decrease (or increase) of the instances of "KTV", which represents the adjustment of an urban regional structure. This result means that Algorithm MDC can find the dynamic relationships among spatial features such as $\{Ganoderma_lucidum_{new}, maple_tree_{dead}\}$.
- 3) The instances of "Hotel", "KTV" and "Bank" always appear/disappear simultaneously, which indicates that they have strong symbiotic relationships, and they reflect the economic prosperity/recession in this region because they denote the level of regional economic development. This result means that Algorithm MDC can effectively avoid the wrong conclusion that the instances of two or more features increase/decrease (i.e., new/dead) in the same/approximate proportion, which has no effect on prevalent patterns.

In conclusion, Algorithm MDC can obtain certain meaningful patterns such as $\{water_hyacinth_{new}(\text{increase}), algae_{dead}(\text{decrease})\}$ and $\{Ganoderma_lucidum_{new}, maple_tree_{dead}\}$, and avoid the wrong conclusion that the instances of two or more features increase/decrease (i.e., new/dead) in the same/approximate proportion, which has no effect on prevalent patterns."

B. Experiments on Synthetic Datasets

In this section, we examine the representation of the prevalent maximal D_c for all prevalent D_c , the efficiency of Algorithm MDC, and the performance of the pruning strategies.

We randomly generate synthetic datasets, where the *time span* is 3, there are 11 time points, and the distribution area of spatial instances is 1000*1000. By default, the number of dynamic instances and dynamic features are 10000 and 10,

respectively; the *life cycle* of all dynamic features is $\{9,3,30,15,27,24,30,3,24,18\}$; and min_prev and D_d are 0.1 and 35, respectively.

1) Change Trend of Maximal D_c and D_c

We analyze the change trend of the number of size- k ($k \in [1,10]$) patterns (i.e., the pattern of each size) and the sum of the number of patterns from size-1 to size- k (i.e., sum of patterns), as shown in Fig. 4.

Furthermore, the change trend of the number of maximal D_c and that of D_c are approximate to the blue line (the pattern of each size) and red line (i.e., sum of patterns), respectively. Suppose both of the size- k patterns and its low-size patterns are prevalent, and the size- $k+1$ patterns are non-prevalent. On the one hand, the subsets of the size- k patterns are prevalent and its superset are non-prevalent at this time, and by the definition of the maximal D_c , the size- k patterns are maximal prevalent patterns, which leads to the observation that the change trend of the number of prevalent maximal D_c is approximate to that of the size- k patterns (i.e., the pattern of each size (blue line)). On the other hand, all prevalent patterns include patterns from size-1 to size- k , which leads to the observation that the change trend of the number of prevalent D_c is approximate to the red line (i.e., sum of patterns). Finally, although the analysis of change trend starts from the supposed premise, its real change trend is actually approximate to the lines shown in Fig. 4.

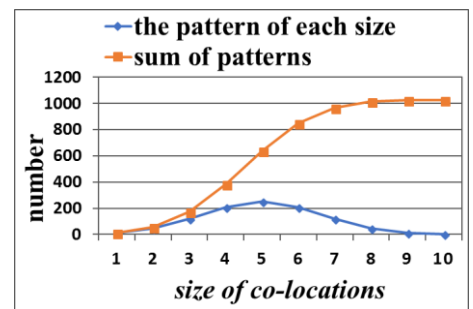


Fig. 4. Change trend of pattern with different size

In Fig. 4, the blue line first increases and subsequently decreases, which represents the change trend of the number of prevalent maximal D_c mined by our method. The red line continues to increase, which represents the change trend of the number of prevalent D_c mined by traditional methods. First, with the increase of size- k , the gap between the number of prevalent maximal D_c and that of prevalent D_c becomes larger, which means that mining the prevalent maximal D_c is more efficient than mining the prevalent D_c . Moreover, with the increase of size- k , the number of prevalent D_c significantly increases, which leads to the observation that the execution time of the traditional method is unacceptable,

and thus we only display the complete trend (i.e., the prevalent maximal D_c first increases and subsequently decreases) in Fig. 5(a), which is treated as a sample example and partial trend (i.e., the prevalent maximal D_c increases) in other comparison experiments.

2) *Representativeness of Prevalent Maximal D_c*

We compare the number of prevalent maximal D_c with the number of prevalent D_c over the change in *number of dynamic instances*, D_d , *min_prev*, and *number of dynamic features*, as shown in Table III, Table IV, Table V and Table VI (Comparisons in Fig. 5 is more intuitive). With the increase in *number of dynamic instances*, the numbers of prevalent maximal D_c and prevalent D_c increase, which lead to the increase of size- k of the prevalent maximal D_c and prevalent D_c such that the number of prevalent maximal D_c first increases and subsequently decreases and that of the prevalent D_c continues to increase, as shown in Fig. 5(a) (or Table III) and Fig. 4.

TABLE III

REPRESENTATIVENESS OF VARIED NUMBER OF DYNAMIC INSTANCES							
dynamic instances	5k	6k	7k	8k	9k	10k	11k
prevalent maximal D_c	99	131	154	191	162	142	99
prevalent D_c	193	270	414	580	670	720	870

TABLE IV

REPRESENTATIVENESS OF VARIED D_d					
D_d	15	20	25	30	35
prevalent maximal D_c	44	73	115	153	170
prevalent D_c	44	101	214	376	583

TABLE V

REPRESENTATIVENESS OF VARIED <i>min_prev</i>					
<i>min_prev</i>	0.25	0.20	0.15	0.10	0.05
prevalent maximal D_c	93	104	116	126	139
prevalent D_c	306	376	460	583	767

TABLE VI

REPRESENTATIVENESS OF VARIED NUMBER OF DYNAMIC FEATURES					
dynamic features	9	10	11	12	13
prevalent maximal D_c	67	152	316	658	1096
prevalent D_c	416	752	1070	2059	3349

Because the execution time of the traditional method is unacceptable, we only display a partial trend (i.e., the prevalent maximal D_c increases) in other comparison experiments (more detailed information is given in the previous section). From Fig. 5(b)(c)(d) (or Table IV, Table V and Table VI), on the one hand, the number of prevalent maximal D_c is far less than the number of all prevalent D_c , which means that mining the prevalent maximal D_c by our method is more efficient than mining the prevalent D_c by traditional methods. On the other hand, with the change of D_d , *min_prev* and *number of dynamic features*, the gap between the number of prevalent maximal D_c and that of

prevalent D_c becomes larger, and the difference in efficiency between mining the prevalent maximal D_c by our method and mining the prevalent D_c by the traditional method is increasingly obvious.

3) *Efficiency of Algorithm MDC*

We compare the running times for mining the prevalent D_c by Algorithm MDC and the join-based algorithm [15,16] over the change in *number of dynamic instances*, D_d , *min_prev* and *number of dynamic features*, as shown in Fig. 6. Because the number of prevalent D_c is small on the original parameters, the advantage of Algorithm MDC is not obvious compared with traditional method. Moreover, with the change in these parameters, the number of prevalent D_c increases, and the difference in efficiency between mining the prevalent maximal D_c by our method and mining the prevalent D_c by the traditional method is becomes more obvious.

4) *Performance of Pruning Strategies*

We compare the efficiency before and after pruning via pruning strategies 1 and 2, which can effectively accelerate the process of mining the prevalent maximal D_c by Algorithm MDC, as shown in Fig. 7.

VIII. CONCLUSION

Because the existing methods cannot mine the dynamic relationships among spatial features, and the number of prevalent patterns is too large, this paper proposes 1) the definition of a dynamic spatial co-location pattern, 2) the idea of mining the prevalent maximal patterns instead of all prevalent patterns (the former can be used to derive the latter), and 3) an algorithm for mining the maximal dynamic spatial co-location patterns (i.e., Algorithm MDC) based on the maximal dynamic feature clique.

Mining the dynamic spatial co-location pattern can remedy the defects of the existing methods. The existing methods miss certain meaningful patterns, such as $\{Ganoderma_lucidum_{new}, maple_tree_{dead}\}$ and $\{water_hyacinth_{new}(increase), algae_{dead}(decrease)\}$, and obtain the wrong conclusion that the instances of two or more features increase/decrease (i.e., new/dead) in the same/approximate proportion, which has no effect on prevalent patterns. Therefore, we propose the dynamic spatial co-location pattern D_c , which can reflect the dynamic relationships among spatial features similar to the above three types of dynamic changes.

Compared with mining the prevalent D_c , mining the prevalent maximal D_c that can derive all prevalent D_c is more efficient. The number of prevalent patterns is large, which makes the efficiency of the existing methods low. Therefore, we introduce the prevalent maximal pattern into the process of mining the prevalent D_c because the prevalent maximal patterns are compact representations of all

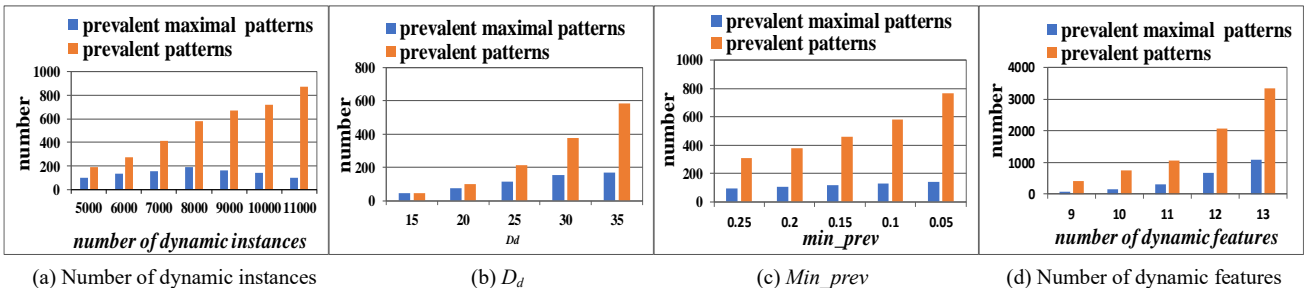


Fig. 5. Representativeness of prevalent maximal D_c

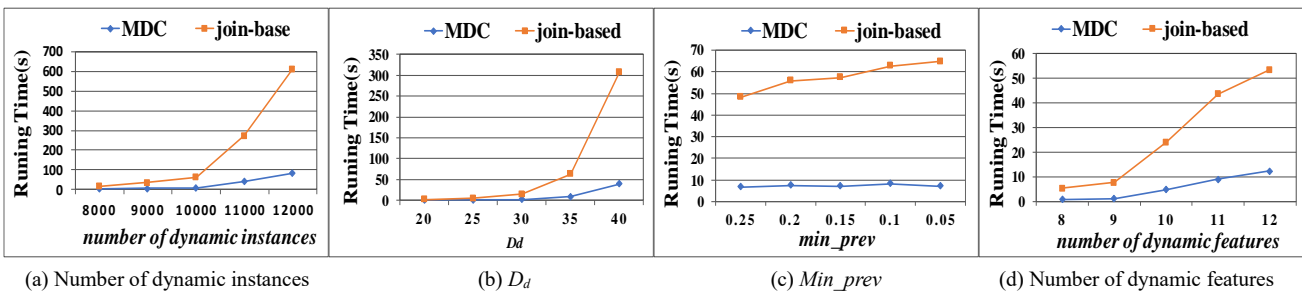


Fig. 6. Efficiency of Algorithm MDC

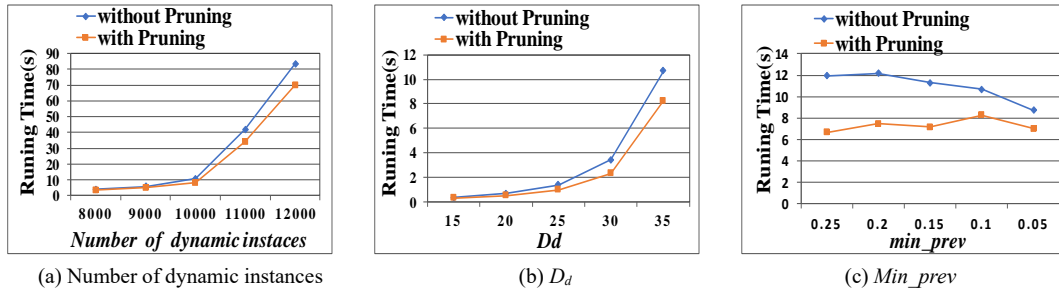


Fig. 7. Performance of pruning strategies

prevalent patterns and can be used to derive all prevalent patterns. The gap between the number of prevalent maximal Dc and that of the prevalent Dc is large, and thus the difference in efficiency between mining the prevalent maximal Dc by our method and mining the prevalent Dc by the traditional method is obvious.

We propose an algorithm (i.e., Algorithm MDC) for mining the prevalent maximal Dc to avoid the many connections and computations in the existing methods. We convert the size-2 prevalent patterns into a dynamic feature graph (DG) by *Algorithm1* such that the calculation and connection for the table instances are turned into the calculation and connection of the dynamic features. We obtain the set of maximal dynamic feature clique Dfc from the dynamic feature graph DG by *Algorithm2*. Finally, the maximal dynamic feature cliques as candidate maximal dynamic spatial co-location patterns are verified by *Algorithm3*, and we can obtain the prevalent maximal Dc . Moreover, we propose two pruning strategies to improve the efficiency of Algorithm MDC.

The experimental results from a real dataset and a synthetic dataset show that our algorithm can effectively mine the prevalent maximal Dc , that the number of prevalent maximal Dc is much less than the number of all prevalent Dc and that the performance of Algorithm MDC is better than the join-based [15,16].

The biggest limitation of our method is that parameters are designated by domain experts, such as Dd , min_prev , $time_span$, which is the common problem of mining spatial co-location pattern and is also the future research directions: 1) parameters might be learned from the dataset that can reduce the subjectivity of the parameter designated by experts as much as possible; 2) methods for how to set a more reasonable $time_span$ can be considered to maximize the value/meaning of the dynamic spatial co-location patterns; 3) more efficient approaches to mining the prevalent maximal dynamic spatial co-location patterns can be designed. Our study also opens the door to exploring the dynamic relationships among spatial features.

REFERENCES

- [1] A. Soltani, M.R. Akbarzadeh-T, "Confabulation-inspired association rule mining for rare and frequent itemsets," *IEEE Trans. Neural Netw.*, vol. 25, no. 11, pp. 2053-2064, 2014.
- [2] B. Wang, K.E. Merrick, H.A. Abbass, "Co-operative coevolutionary neural networks for mining functional association rules," *IEEE Trans. Neural Netw.*, vol. 28, no. 6, pp. 1331-1344, 2017.
- [3] X. Zhao, N. Evans, J. L. Dugelay, "A subspace co-training framework for multi-view clustering," *Pattern Recognit. Lett.*, vol. 41, pp. 73-82, 2014.
- [4] Y. Jiang, F. L. Chung, S. Wang, et al., "Collaborative fuzzy clustering from multiple weighted views," *IEEE T. Cybern.*, vol.45, no.4, pp. 688-701, 2014.
- [5] M. White, X. Zhang, D. Schuurmans, et al., "Convex multi-view subspace learning," in *Proc. NIPS*, 2012, pp. 1673-1681.
- [6] Y. Jiang, F. L. Chung, H. Ishibuchi, et al., "Multitask TSK fuzzy system modeling by mining intertask common hidden structure," *IEEE T. Cybern.*, vol. 45, no. 3, pp. 534-547, 2014.
- [7] J. Li, A. Adilmagambetov, M.S.M. Jabbar, et al., "On discovering co-location patterns in datasets: a case study of pollutants and child cancers," *Geoinformatica*, vol. 20, no. 4, pp. 651-692, 2016.
- [8] S. An, H. Yang, J. Wang, et al., "Mining urban recurrent congestion evolution patterns from GPS-equipped vehicle mobility data," *Inf. Sci.*, vol. 373, no. 10, pp. 515-526, 2016.
- [9] W. Yu, "Spatial co-location pattern mining for location-based services in road networks," *Expert Syst. Appl.*, vol. 46, pp. 324-335, 2016.
- [10] M. Akbari, F. Samadzadegan, R. Weibel, "A generic regional spatio-temporal co-occurrence pattern mining model: a case study for air pollution," *J. Geogr. Syst.*, vol. 17, pp. 249-274, 2015.
- [11] X. Song, L. Nie, L. Zhang, et al., "Interest inference via structure-constrained multi-source multi-task learning," In *Proc. IJCAI*, 2015, pp. 2371-2377.
- [12] J. Zhang, L. Nie, X. Wang, et al., "Shorter-is-Better: Venue category estimation from micro-video," in *Proc. ACM Multimedia*, 2016, pp. 1415-1424.
- [13] X. Chang, Z. Ma, M. Lin, et al., "Feature Interaction Augmented Sparse Learning for Fast Kinect Motion Detection," *IEEE Trans. Image Process.*, vol. 26, no. 8, pp. 3911-3920, 2017.
- [14] X. Wang YL, Zhao, L. Nie, et al., "Semantic-Based Location Recommendation With Multimodal Venue Semantics," *IEEE Trans. Multimedia*, vol. 17, no. 3, pp. 409-419, 2015.
- [15] X. Chang, Z. Ma, Y. Yi, et al., "Bi-Level Semantic Representation Analysis for Multimedia Event Detection," *IEEE Trans. Cybern.*, vol. 47, no. 5, pp. 1180-1197, 2017.
- [16] Z. Ma, X. Chang, Y. Yang, et al., "The Many Shades of Negativity," *IEEE Trans. Multimedia*, vol. 19, no. 7, pp. 1558-1568, 2017.
- [17] L. Zhu, Z. Huang, X. Liu, et al., "Discrete multi-modal hashing with canonical views for robust mobile landmark search," *IEEE Trans.*

- Multimedia*, vol. 19, no. 9, pp. 2066–2079, 2017.
- [18] L. Zhu, J. Shen, H. Jin, et al., “Landmark classification with hierarchical multi-modal exemplar feature,” *IEEE Trans. Multimedia*, vol. 17, no. 7, pp. 981-993, 2015.
- [19] L. Zhu, J. Shen, X. Liu, et al., “Learning compact visual representation with canonical views for robust mobile landmark search,” in *Proc. IJCAI*, 2016, pp. 3959-3967.
- [20] S. Shekhar, Y. Huang, “Colocation rules mining: a summary of results,” *Biochem. Biophys. Res. Commun.*, vol. 414, no. 2, pp. 355-360, 2011.
- [21] L. Wang, H. Chen, “Theory and method of spatial pattern mining,” Beijing, China: Science Press, 2014, pp. 95-106.
- [22] J. Zhao, L. Wang, P. Yang, et al. “Mining High Utility Co-location Patterns Based on Importance of Spatial Region,” in *proc. International Conference on Geo-Spatial Knowledge and Intelligence*, 2017, pp. 43-55.
- [23] L. Wang, W. Jiang, H. Chen, Y. Fang, “Efficiently mining high utility co-location patterns from spatial data sets with instance-specific utilities,” in *Proc. DASFAA*, 2017, pp. 458-474.
- [24] S. Yang, L. Wang, X. Bao, et al., “A framework for mining spatial high utility co-location patterns,” in *Proc. FSKD*, 2015, pp.631-637.
- [25] L. Wang, X. Bao, L. Zhou, “Redundancy reduction for prevalent co-location patterns,” *IEEE Trans. Knowl. Data Eng.*, vol. 30, no. 1, pp. 142-155, 2018.
- [26] W. Andrzejewski, P. Boinski, “Efficient spatial co-location pattern mining on multiple GPUs,” *Expert Syst. Appl.*, vol. 93, pp. 465-483, 2018.
- [27] J. Lu, L. Wang, Y. Fang, “Mining causal rules hidden in spatial co-locations based on dynamic spatial databases” in *Proc. CITS*, 2016, pp. 1-6.
- [28] J. Lu, L. Wang, Y. Fang, et al. “Mining competitive pairs hidden in co-location patterns from dynamic spatial databases,” in *Proc. PAKDD*, 2017, pp. 467-480.
- [29] Z. Ouyang, L. Wang, P. Wu, “Spatial co-location pattern discovery from fuzzy objects,” *Int. J. Artif. Intell. Tools*, vol. 26, no. 2, pp. 1-20, 2017.
- [30] L. Wang, P. Wu P, H. Chen, “Finding Probabilistic Prevalent Colocations in Spatially Uncertain Data Sets”, *IEEE Trans. Knowl. Data Eng.*, vol. 25, no. 4, pp. 790-804, 2013.
- [31] Z. Liu, Y. Huang, “Mining co-locations under uncertainty,” in *Proc. SSTD*, 2013, pp. 429-446.
- [32] M. Sheshikala, D. Rajeswara Rao, and Md. Ali Kadampur, “Co-location Data Mining on Uncertain Datasets Using a Probabilistic Approach,” *International Journal of Applied Engineering Research*, vol. 10, no.12, pp. 31269-31280, 2015.
- [33] L. Wang, J. Han, H. Chen, et al., “Top-k probabilistic prevalent co-location mining in spatially uncertain data sets,” *Frontiers of Computer Science*, vol. 10, no. 3, pp. 488-503, 2016.
- [34] V. Kavi, D. Joshi, “A survey on enhancing data processing of positive and negative association rule mining,” *International Journal of Computer Sciences and Engineering*, vol. 2, no. 3, pp. 139-143, 2014.
- [35] R. Sethi, B. Shekar, “Issues in negative association rule mining with business analytics perspectives,” *DHARANA-Bhavan's International Journal of Business*, vol. 11, no. 2, pp. 13-20, 2018.
- [36] D. Liu, H. Chen, H. Qi, et al., “Advances in spatio-temporal data mining,” *Journal of Computer Research & Development*, vol. 50, no. 2, pp. 225-239, 2013.
- [37] N. Yusof, R. Zurita-Milla, “Mapping frequent spatio-temporal wind profile patterns using multi-dimensional sequential pattern mining,” *Int. J. Digit. Earth*, vol. 10, no. 3, pp. 238-256, 2017.
- [38] J. Lu, L. Wang, Y. Fang, et al. “Mining Strong Symbiotic Patterns Hidden in Spatial Prevalent Co-location Patterns,” *Knowledge-Based Syst.*, vol. 146, pp. 190-202, 2018.
- [39] L. Wang, L. Zhou, J. Lu, J. Yip, “An Order-clique-based Approach for Mining Maximal Co-location pattern,” *Inf. Sci.*, vol. 179, pp. 3370-3382, 2009.
- [40] X. Yao, L. Peng, L. Yang, et al. “A fast space-saving algorithm for maximal co-location pattern mining,” *Expert Syst. Appl.*, vol. 63, pp. 310-323, 2016.
- [41] X. Yao, D. Wang, L. Peng, et al. “An adaptive maximal co-location mining algorithm,” in *Proc. IJARSS*, 2017, pp. 5551-5554.
- [42] B. Dai and M. Lin, “Efficiently Mining Dynamic Zonal Co-Location Patterns based on Maximal Co-location pattern,” in *Proc. ICDM*, 2011, pp. 861-868.

- [43] X. Bao, L. Wang, J. Zhao, “Mining top-k-size maximal co-location patterns,” in *Proc. CITS*, 2016, pp. 1-6.
- [44] L. Wang, X. Bao, L. Zhou, et al, “Maximal Sub-prevalent Co-location Patterns and Efficient Mining Algorithms,” in *Proc. WISE*, 2017, pp.199-214.
- [45] X. Hu, L. Wang, et al., “Degree-based approach for the maximum clique problem,” *Journal of Frontiers of Computer Science and Technology*, vol. 7, no. 3, pp. 262-271, 2013.
- [46] X. Hu, L. Wang, L. Zhou, et al. “Mining spatial maximal co-location patterns,” *Journal of Frontiers of Computer Science and Technology*, vol. 8, no. 2, pp. 150-160, 2014.



Xin Hu was born in Mianyang, China in 1988. He received the B.S. degree in computer science and technology from Capital Normal University, Beijing, China, in 2011, M.S degree in computer application technology from Yunnan University, Kunming, Yunnan, China, in 2014 and PhD degree in computer application technology from Beijing

Normal University, Beijing, China, in 2019.

He is an assistant professor of Yangtze Normal University. His main research interests include knowledge graph, question answering, data mining, crowdsourcing.



Guoyin Wang (SM'03) received the B.S., M.S., and Ph.D. degrees from Xi'an Jiaotong University, Xi'an, China, in 1992, 1994, and 1996, respectively. He was at the University of North Texas, and the University of Regina, Canada, as a visiting scholar during 1998-1999.

Since 1996, he has been at the Chongqing University of Posts and Telecommunications, where he is currently a professor, the director of the Chongqing Key Laboratory of Computational Intelligence, and the dean of the School of Graduate. He was appointed as the director of the Institute of Electronic Information Technology, Chongqing Institute of Green and Intelligent Technology, CAS, China, in 2011. He is the author of 10 books, the editor of dozens of proceedings of international and national conferences, and has more than 200 reviewed research publications. His research interests include rough set, granular computing, knowledge technology, data mining, neural network, and cognitive computing.

Prof. Wang is a senior member of the IEEE.



Jiangli Duan was born in 1989. She received the B.S. and M.S. degrees from Yunnan University, Kunming, Yunnan, China, in 2012 and 2017. She is currently pursuing the PhD degree in computer science and technology at Chongqing University of Posts and Telecommunications, Chongqing, China.

She is also an assistant professor of Yangtze Normal University, Chongqing, China. Her main research interests include knowledge graph, question answering, data mining, granular computing and cognitive computing.